

TOMOGRAPHIC IMAGE RECONSTRUCTION FROM LIMITED-VIEW PROJECTIONS WITH WIENER FILTERED FOCUSS ALGORITHM

Rafal Zdunek

Institute of Telecommunications,
Teleinformatics, and Acoustics
Wroclaw University of Technology
Wybrzeze Wyspianskiego 27
50-370 Wroclaw, Poland
E-mail: rafal.zdunek@pwr.wroc.pl

Zhaoshui He*, Andrzej Cichocki†

Lab. for Advanced Brain Signal Processing
RIKEN Brain Science Institute
2-1 Hirosawa, Wako-shi
Saitama 351-0198, Japan
E-mails: he_shui@brain.riken.jp
cia@brain.riken.jp

ABSTRACT

In tomographic image reconstruction from limited-view projections the underlying inverse problem is ill-posed with the rank-deficient system matrix. The minimal-norm least squares solution may considerably differs from the true solution, and hence a priori knowledge is needed to improve the reconstruction. In our approach, we assume that the true image presents sparse features with uniform spacial smoothness. The sparsity constraints are imposed with the ℓ_p diversity measure that is minimized with the FOCUSS algorithm. The spacial smoothness is enforced with the adaptive Wiener noise removing implemented in each FOCUSS iterations. The simulation results demonstrate the benefits of the proposed approach.

Index Terms— Tomographic image reconstruction, Limited data tomography, FOCUSS algorithm, Wiener noise removing, Rank-deficient inverse problems

1. INTRODUCTION

When an angular range of projections in tomographic image reconstruction is limited, the reconstructed images are distorted with specific smeared artifacts that are often called "ghosts" in the literature [1, 2]. Koltracht et al. [2] proved that for borehole tomography (limited-view projections), the nullspace of the forward projection operator is non-trivial, which implies the non-unique inversion, and in consequence the minimal-norm least-square solution may not be the true solution.

In many cases of limited-view image reconstruction, the ambiguity of the inversion and related artifacts are reduced by suitable regularization that stabilizes the solution or improves

it with some prior information. However, efficient regularization of the solution is a very challenging task, and it requires careful treatment of the prior information. In many cases, the prior knowledge on the solution is limited, e.g. only to a degree of smoothness or sparsity. In our approach we take advantage of both kinds of prior information. The sparsity constraints are imposed by using the ℓ_p diversity measure as a regularization term, which leads to the FOCUSS algorithm. The smoothness constraints are imposed by the adaptive Wiener noise removing (filtration) from each iterative updates with the FOCUSS algorithm. This modification is easy to implement and the related smoothness parameter can be readily estimated.

2. MODEL

Assuming the forward projection model as the limited angle Radon transform, a discrete approximation of the model can be expressed by

$$\mathbf{A}\mathbf{x} + \mathbf{n} = \mathbf{b}, \quad (1)$$

where $\mathbf{A} = [a_{ij}] \in \mathbb{R}^{M \times N}$ is the system matrix, $\mathbf{x} = [x_j] \in \mathbb{R}^N$ is the unknown image vector, $\mathbf{n} = [n_i] \in \mathbb{R}^M$ is the vector of errors or noisy perturbations, and $\mathbf{b} = [b_i] \in \mathbb{R}^M$ is the vector of observations. The area of interest is uniformly discretized into N square pixels, and probed along M ray-paths (projections). We assume that the angular range of the projections is limited to $[0, \pi/2]$, and this implies $\text{rank}(\mathbf{A}) < \min\{M, N\}$ in spite of $M \geq N$. Each entry a_{ij} represents the contribution of the i -th ray-path to the j -th pixel.

Since the angular range of projections is considerably limited, the inverse problem is severely ill-posed and the nullspace $N(\mathbf{A})$ is not trivial. Any solution \mathbf{x}_* to the least square problem $\min_{\mathbf{x}} \|\mathbf{b} - \mathbf{A}\mathbf{x}\|_2^2$ can be expressed as $\mathbf{x}_* = \mathbf{x}_{LS} + \mathbf{x}_n$ where \mathbf{x}_{LS} is the unique minimal-norm least squares solution, which is generally non-sparse, and $\mathbf{x}_n \in N(\mathbf{A})$ represents any linear combination of the

*School of Electronics and Information Engineering, South China University of Technology, Guangzhou 510641, China

†System Research Institute, Polish Academy of Sciences (PAN); and Department of EE; Warsaw University of Technology; Warsaw, Poland

nullspace vectors. Thus some prior knowledge on the true solution is needed to give preference to a certain class of the solutions. Assuming the true image contains sparse features, the sparsity constraints can be imposed to select the right solution.

3. ALGORITHMS

A variety of computational strategies exists for finding sparse solutions to systems of linear equations. Examples include the BP [3], greedy algorithms [4], Iterative-Thresholding algorithms [5], FOCUSS algorithm [6] and its extensions such as FOCUSS-CNDL [7] or LORETA-FOCUSS [8].

The FOCUSS, which is based on Iteratively Reweighted Least Square (IRLS) algorithm [9], has already found numerous applications in neuro-imaging such as EEG/MEG [10], where the inverse problems are linear, under-determined and sparse. From a mathematical point of view such inverse problems have similar numerical properties (at least in the sense of a non-trivial nullspace) as linear rank-deficient problems, and this motivates the usage of the FOCUSS to image reconstruction from limited-view projections.

3.1. Regularized FOCUSS algorithm

The problem of finding the sparse solution to the system (1) can be formulated in terms of the following regularized least-squares problem:

$$\min_x \|Ax - b\|_2^2 + \gamma E^{(p)}(x) \quad (2)$$

where γ controls a tradeoff between fitting to data and sparsity, and

$$E^{(p)} = \text{sgn}(p) \sum_{j=1}^N |x_j|^p, \quad p \leq 1, \quad (3)$$

is the ℓ_p diversity measure [6]. The parameter p affects a degree of sparsity in x .

The regularized FOCUSS algorithm iteratively seeks stationary points of the objective function in (2) using the IRLS algorithm [9]. The final form of the FOCUSS is given by Algorithm 1 where $\lambda = \frac{|p|}{2}\gamma$ is a regularization parameter, and $I_M \in \mathbb{R}^{M \times M}$ is an identity matrix.

3.2. Spatial smoothness constraints

The adaptive Wiener filtration [11] has been extensively used in tomographic image reconstruction [12–14] to remove a constant power Gaussian white noise. An example of using the Wiener filtration for extracting brain evoked potentials can be found in [15].

We propose to remove noisy disturbances from each iterative update $x^{(k+1)}$ using the pixelwise adaptive lowpass

Algorithm 1 (Regularized FOCUSS)

Set $p \in [0, 2]$, % p -norm,
 λ % regularization parameter,
 Randomly initialize $x^{(0)}$,
For $k = 1, 2, \dots$, until convergence **do**
 $W_k = \text{diag} \{(|x_j|^{(k)})^{1-\frac{p}{2}}\}$,
 $x^{(k+1)} = W_k^2 A^T (A W_k^2 A^T + \lambda I_M)^{-1} b$,
End

Wiener filter as follows

$$x_j^{(k+1)} \leftarrow \mu_j + \frac{\sigma_j^2 - \nu_j^2}{\sigma_j^2} (x_j^{(k+1)} - \mu_j), \quad (4)$$

$$\mu_j = \frac{1}{L-1} \sum_{n \in N_j} x_n^{(k+1)},$$

$$\sigma_j^2 = \frac{1}{L-1} \sum_{n \in N_j} ((x_n^{(k+1)})^2 - \mu_j^2),$$

where μ_j and σ_j^2 are the local mean and variance around the j -th pixel, respectively. The set N_j contains the indices of the neighboring pixels around the j -th pixel, L is the total number of pixels in the neighborhood, and ν^2 is the mean noise variance which is calculated as follows:

$$\nu^2 = \frac{1}{N} \sum_{j=1}^N \sigma_j^2. \quad (5)$$

The nearest neighborhood N_j can be defined with the Markov Random Field (MRF) model. Assuming the first- and second-order interactions between cliques of pixels, we have $L = 9$. In the experiments, we used the Wiener filter implemented in Image Processing Toolbox from MATLAB 7.0.

4. RESULTS

In the simulation experiments we used the synthetic data from borehole tomography [16] which is commonly used to identify anomalies in the geophysical structure of a cross-borehole section. The anomalies may result both from human activity or natural lithologic processes, and are expected to be sparse and smooth. An exemplary discrete representation of the borehole tomographic image (phantom) is shown in Fig. 1(a). The area is divided into 64 by 64 pixels, hence $N = 4096$. The observations are obtained using regular cross-borehole probing of the area of interest. The total number of the probing ray-paths amounts to 4096. Thus $A \in \mathbb{R}^{4096 \times 4096}$.

Since an angular range of the probing ray-paths is strongly limited, the observations may be incomplete. The numerical rank of A evaluated in MATLAB 7.0 is equal to 3658.

The minimal norm least squares solution (\mathbf{x}_{LS}) obtained by orthogonal projection of the lexicographically vectorized true image onto $N(\mathbf{A})$ is illustrated in Fig. 1(b). Note that the standard ART, SIRT, LSQR, or CGLS algorithms are convergent to \mathbf{x}_{LS} only for consistent (noise-free) data. For noisy data, the approximations obtained with these algorithms would be even worse.

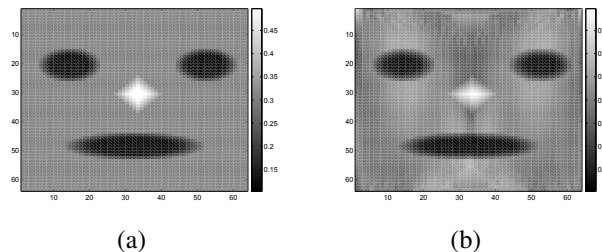


Fig. 1. (a) Phantom image; (b) Minimal-norm least-squares solution.

To reconstruct the image we used the standard and Wiener filtered FOCUSS algorithms. Since the sparse reconstructed images are also expected to be smooth, the parameter p should not be equal to zero because this may cause the algorithm easily gets stuck to local minima of the non-convex objective function in (2). We propose to choose typically $p = 1$, which is equivalent to solving an equality constrained l_1 problem. However, Linear Programming (LP) cannot be readily applied here because our l_1 problem is degenerate (\mathbf{A} does not have a full rank). For example, the large-scale primal-dual interior-point method (Matlab's optimization toolbox) which is a variant of the Mehrotra's predictor-corrector algorithm cannot give satisfactory results for our problems. The algorithms are tested with noise-free and zero-mean Gaussian noisy data with $SNR = 30$ [dB].

The images reconstructed with both algorithms within 15 iterations are shown in Fig. 2. The regularization parameter λ for noisy data has been estimated with the L-curve based method given in [17]. For noise-free data we set λ to its lowest boundary. The reconstructed images are also estimated quantitatively with the standard Root Mean Square Error (RMSE) plotted in Fig. 3 versus the number of iterations.

Inclusion of the Wiener filtering to the FOCUSS iterations nearly does not affect a total computational cost which is mostly caused by a matrix inversion in the FOCUSS algorithm. Obviously, this step can be relaxed by using linear iterative solvers to approximate the term $(\mathbf{A}\mathbf{W}_k^2\mathbf{A}^T + \lambda\mathbf{I}_M)^{-1}\mathbf{b}$. We applied the Gaussian elimination in this step to get an exact results. According to Matlab evaluation of elapsed time one iterative step of the FOCUSS algorithm with and without the Wiener filtration amounts to about 33.8 and 33.6 seconds, respectively. The algorithms have been tested in Matlab 7.0 on PC (1GB RAM, Dual Core CPU, 1.7 GHz).

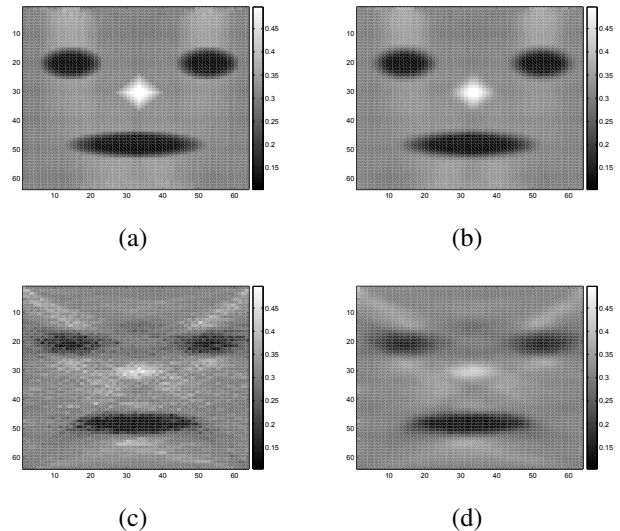


Fig. 2. Images reconstructed with FOCUSS ($p = 1$, $k = 15$): (a) noise-free data and without filtering, $\lambda = 10^{-8}$; (b) noise-free data and with adaptive Wiener filtering, $\lambda = 10^{-8}$; (c) noisy data ($SNR = 30$ [dB]) and without filtering, $\lambda = 40$; (d) noisy data ($SNR = 30$ [dB]) and with adaptive Wiener filtering, $\lambda = 40$.

5. CONCLUSIONS

In the paper, we propose to use the FOCUSS algorithm with the adaptive Wiener filtering to enforce additional smoothness constraints. As shown in Fig. 2(a) the image reconstructed from noise-free data using the standard FOCUSS has a little better quality (with relaxed vertical smearing artifacts) than the solution \mathbf{x}_{LS} shown in Fig. 1(b). The usage of the Wiener filtering [see Fig. 2(b)] enforces the image to be smoother (for $p = 1$), and in this theoretical (noise-free) case the filtering is unnecessary. For smaller values of p , the filtering gives some slight improvements as shown in Fig. 3(a). However, if the data are noisy (real data), the Wiener filtering is very important and considerably improves the reconstruction – compare Fig. 2(c) (without filtering) with Fig. 2(d) (with filtering), and also Fig. 3(b).

6. REFERENCES

- [1] N. D. Bregman, R. C. Bailey, and C. H. Chapman, "Ghosts in tomography: The effect of poor angular coverage in 2-D seismic traveltime inversion," *Canadian J. Expl. Geophysics*, vol. 25, pp. 7–27, 1989.
- [2] I. Koltracht, P. Lancaster, and D. Smith, "The structure of some matrices arising in tomography," *Linear Algebra and Its Applications*, vol. 130, pp. 193–218, 1990.

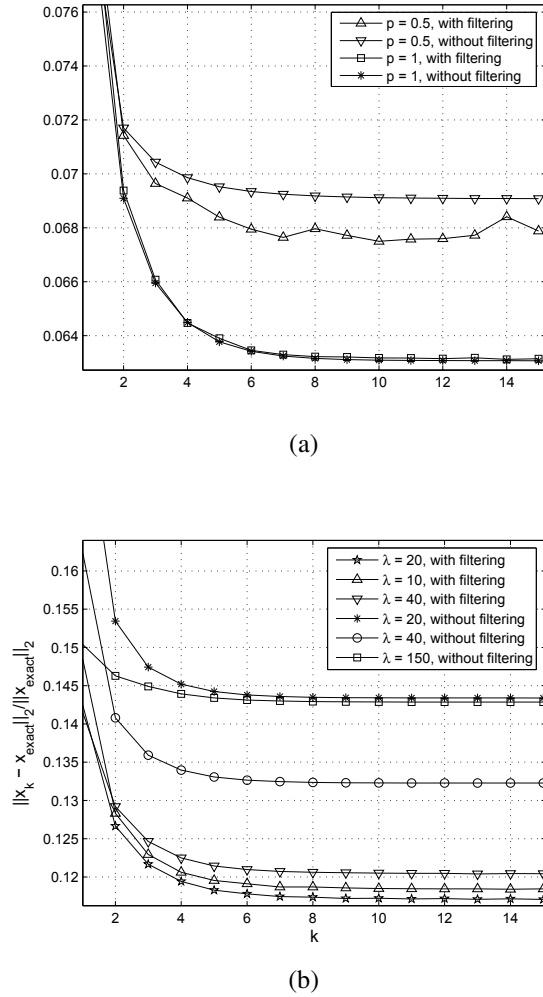


Fig. 3. Normalized RMSE versus the number of iterations: (a) noise-free data; (b) noisy data ($SNR = 30$ [dB]).

- [3] S. S. Chen, D. L. Donoho, and M. A. Saund, "Atomic decomposition by basis pursuit," *SIAM Journal on Scientific Computing*, vol. 20, no. 1, pp. 33–61, 1998.
- [4] J. A. Tropp, A. C. Gilbert, and M. J. Strauss, "Algorithms for simultaneous sparse approximation, part I: Greedy pursuit," *Signal Processing*, vol. 86, no. 3, pp. 572–588, 2006.
- [5] I. Daubechies, M. Defrise, and C. De Mol, "An iterative thresholding algorithm for linear inverse problems with a sparsity constraint," *Communications on Pure and Applied Mathematics*, vol. 57, no. 11, pp. 1413–1457, 2004.
- [6] I. F. Gorodnitsky and B. D. Rao, "Sparse signal reconstructions from limited data using FOCUSS: A re-weighted minimum norm algorithm," *IEEE Trans. Signal Processing*, vol. 45, pp. 600–616, March 1997.
- [7] J. F. Murray and K. Kreutz-Delgado, "Learning sparse overcomplete codes for images," *The Journal of VLSI Signal Processing*, vol. 45, no. 1–2, pp. 97–110, November 2006.
- [8] H. Liu, P. H. Schimpf, G. Dong, X. Gao, F. Yang, and S. Gao, "Standardized shrinking LORETA-FOCUSS (SSLOFO): a new algorithm for spatio-temporal EEG source reconstruction," *IEEE Transactions on Biomedical Engineering*, vol. 52, no. 10, pp. 1681–1691, October 2005.
- [9] L. A. Karlovitz, "Construction of nearest points in the l^p , p even and l^∞ norms," *Journal of Approximation Theory*, vol. 3, pp. 123–127, 1970.
- [10] J. Han and K. S. Park, "Regularized FOCUSS algorithm for EEG/MEG source imaging," in *26th Annual International Conference of the IEEE Engineering in Medicine and Biology Society*, San Francisco, USA, 1993, vol. 1.
- [11] S. J. Lim, *Two-Dimensional Signal and Image Processing*, Prentice Hall, Englewood Cliffs, NJ, 1990.
- [12] Y. Noguchi Y. Funama and M. Shimamura, "Reduction of artifacts in degraded CT image by adaptive Wiener filter," *Jpn. J. Med. Electron. Biol. Eng.*, vol. 40, no. 1, pp. 1–6, 2002.
- [13] A. Ozcan, A. Bilenca, A. E. Desjardins, B. E. Bouma, and G. J. Tearney, "Speckle reduction in optical coherence tomography images using digital filtering," *J. Opt. Soc. Am. A*, vol. 24, no. 7, pp. 1901–1910, 2007.
- [14] A. Pralat and R. Zdunek, "Regularized image reconstruction in electromagnetic geotomography through use of Wiener filter," in *Proc. Conference on Mathematical Methods in Electromagnetic Theory (MMET'2000)*, Kharkov, Ukraine, September 12–15 2000, vol. 2, pp. 607–609.
- [15] A. Cichocki, R. R. Gharieb, and T. Hoya, "Efficient extraction of evoked potentials by combination of Wiener filtering and subspace methods," in *Proc. 2001 IEEE International Conference on Acoustics, Speech, and Signal Processing (ICASSP-2001)*, Salt Lake City, Utah, USA, May 2001, vol. 5, pp. 3117–3120.
- [16] A. Pralat and R. Zdunek, "Electromagnetic geotomography – selection of measuring frequency," *IEEE Sensors Journal*, vol. 5, no. 2, pp. 242–250, 2005.
- [17] B. D. Rao, K. Engan, S. F. Cotter, J. Palmer, and K. Kreutz-Delgado, "Subset selection in noise based on diversity measure minimization," *IEEE Trans. Signal Processing*, vol. 51, no. 3, pp. 760–770, March 2003.